

UAV Assisted Public Safety Communications with LTE-Advanced HetNets and FeICIC

Abhaykumar Kumbhar^{1,2}, Simran Singh³, and İsmail Güvenç³

¹Department of Electrical and Computer Engineering, Florida International University, Miami, FL 33174

²Motorola Solutions, Inc., Plantation, FL 33322 USA

³North Carolina State University, 890 Oval Dr, Raleigh, NC 27606, USA

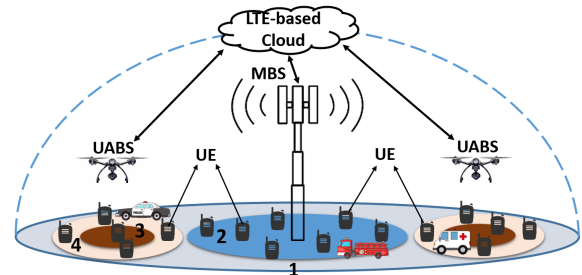
Abstract—Establishing a reliable communication infrastructure at an emergency site is a crucial task for mission-critical and real-time public safety communications (PSC). To this end, use of the unmanned aerial vehicles (UAVs) has recently received extensive interest for PSC to establish reliable connectivity in a heterogeneous network (HetNet) environment. These UAVs can be deployed as unmanned aerial base stations (UABSs) as a part of HetNet infrastructure. In this article, we explore the role of agile UABSs in LTE-Advanced HetNets by applying 3GPP Release 11 further-enhanced inter-cell interference coordination (FeICIC) and cell range expansion (CRE) techniques. Through simulations, we compare the system-wide 5th percentile spectral efficiency (SE) when UABSs are deployed in a hexagonal grid and when their locations are optimized using a genetic algorithm, while also jointly optimizing the CRE and the FeICIC parameters. Our simulation results show that at optimized UABS locations, the 3GPP Release 11 FeICIC with reduced power subframes can provide considerably better 5th percentile SE than the 3GPP Release 10 with almost blank subframes.

Index Terms—Cell range expansion, drone, eICIC, FeICIC, FirstNet, genetic algorithm, interference management, public safety, unmanned aerial vehicles, unmanned aerial base stations.

I. INTRODUCTION

Public safety communications (PSC) is considered to be the cornerstone of public safety response system and plays a critical role in saving lives, property, and national infrastructure during a natural or man-made emergency. The legacy PSC technologies are designed predominantly for delivering mission-critical voice communications over narrowband channels, which have been so far met by operating in the pre-defined channelized spectrum allocation. However, the evolution of data and video applications demands higher channel capacity and improved spectral efficiency (SE) [1], [2].

To enhance the capabilities of next generation broadband PSC networks, recently, FirstNet in the United States is building a 4G Long Term Evolution (LTE) based coast-to-coast public safety network deployed in the 700 MHz band [1]. Similarly, the United Kingdom plans to replace the TETRA system, which currently provides mission-critical communications for public safety agencies and other government organizations, with LTE by the year 2020 [3]. The 4G mobile networks as considered in these examples have great potential to revolutionize PSC during emergency situations by providing high-speed real-time video and multimedia services along with mission-critical communication. Furthermore, LTE-Advanced capabilities such as small cell deployment, interference coordi-



1: MBS without destroyed sequence. 2: MBS with destroyed sequence. 3: UABS without range expansion. 4: UABS with range expansion.

Fig. 1. The PSC scenario with MBS and UABSs constituting a HetNet infrastructure. The UABSs can dynamically change their position to provide an optimal coverage and can utilize range expansion bias to offload MBS UEs.

nation, and cell range extension can restore or extend coverage beyond the existing or damaged PSC networks.

Unmanned aerial base stations (UABSs) such as balloons, quadcopters, and gliders equipped with LTE-Advanced capabilities can be utilized for emergency restoration and temporary expansion of public safety network in case of disaster recovery [4]. These UABSs can be deployed with minimum interdependencies, at low cost, and provide virtually omnipresent coverage which is essential for first-responders to be efficient and save lives. The FirstNet PSC network requires 95% geographical coverage of the country, which will be difficult to achieve using only dedicated cell towers. The UABSs can be deployed when necessary to help achieve this coverage goal. On the other hand, the UABSs may also introduce significant interference problems with the ground network [5]–[7].

Recent studies in the literature [8]–[10] have addressed the application of UABSs for rendering mission-critical communication. However, in a heterogeneous network (HetNet) environment, the performance of these UABSs is limited due to the high inter-cell interference. The effectiveness of 3GPP Release-10 and Release-11 inter-cell interference coordination (ICIC) techniques for fixed HetNet deployments has been studied in the literature [7], while the use of cell range expansion (CRE) for offloading users from a macrocell to UABSs has been explored in [6] without considering ICIC. To our best knowledge, the effectiveness of 3GPP Release-10/11 techniques along with CRE and UABS mobility have not been evaluated in the literature, and such an evaluation is the main goal of this paper. We consider an LTE band class 14 PSC network [1] as shown in Fig. 1; by randomly removing

macro base stations (MBSs), we simulate a mock emergency situation to study the impact of interference and CRE when the UABS are deployed. Subsequently, we explore potential gains in 5th percentile SE (5pSE) from the use of Release-10/11 ICIC techniques for a UABS based PSC network.

The rest of this paper is organized as follows. In Section II, we provide the UABS-based HetNet model, assumptions, and definition of 5pSE as a function of network parameters. The UABSs deployment and ICIC parameter configurations using the genetic algorithm and hexagonal grid UABS model are described in Section III. In Section IV, we analyze and compare the 5pSE of the HetNet using extensive computer simulations for various ICIC techniques, and finally the last section provides some concluding remarks.

II. SYSTEM MODEL

We consider a two-tier HetNet deployment with MBSs and UABSs as shown in Fig. 1, where all the MBSs and UABS locations are captured in matrices \mathbf{X}_{mbs} ($N_{\text{mbs}} \times 2$) and \mathbf{X}_{uabs} ($N_{\text{uabs}} \times 2$), respectively, where N_{mbs} and N_{uabs} denote the number of MBSs and UABSs within the simulation area, and UABSs are deployed at a fixed height. The MBS and user equipment (UE) locations are each modeled using a two-dimensional Poisson point process (PPP) with intensities λ_{mbs} and λ_{ue} , respectively [7], [11]. The UABSs are deployed either at fixed locations in a hexagonal grid or the locations are optimized using the genetic algorithm. We assume that the MBSs and the UABSs share a common transmission bandwidth, round robin scheduling is used in all downlink transmissions, and full buffer traffic is used in every cell. The transmit power of the MBS and UABS are P_{mbs} and P_{uabs} , respectively, while K and K' are the attenuation factors due to geometrical parameters of antennas for the MBS and the UABS, respectively. Then, the effective transmit power of the MBS is $P'_{\text{mbs}} = KP_{\text{mbs}}$, while the effective transmit power of the UABS is $P'_{\text{uabs}} = K'P_{\text{uabs}}$.

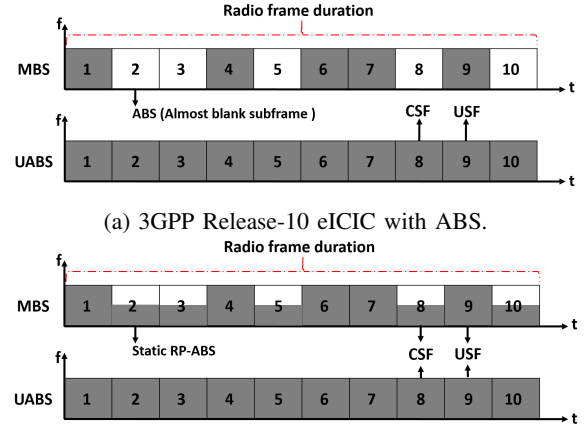
An arbitrary UE n is always assumed to connect to the nearest MBS or UABS, where $n \in \{1, 2, \dots, N_{\text{ue}}\}$. Let the nearest macro-cell of interest (MOI) be at a distance d_{mn} and the nearest UAV-cell of interest (UOI) be at a distance d_{un} . Then, for the n th UE the reference symbol received power from the MOI and the UOI are given by [7]

$$S_{\text{mbs}}(d_{mn}) = \frac{P'_{\text{mbs}}}{d_{mn}^{\delta}}, \quad S_{\text{uabs}}(d_{un}) = \frac{P'_{\text{uabs}}}{d_{un}^{\delta}}, \quad (1)$$

where δ is the path-loss exponent, and d_{un} depends on the locations of the UABSs that will be dynamically optimized.

A. 3GPP Release-10/11 Inter-Cell Interference Coordination

Due to their low transmission power, the UABSs are unable to associate a larger number of UEs compared to that of MBSs. However, by using the cell range expansion (CRE) technique defined in 3GPP Release 8, UABSs can associate a large number of UEs by offloading traffic from MBSs. A negative effect of CRE includes increased interference in the downlink on cell-edge UEs or the UEs in CRE region of the UABS, which is addressed by using ICIC techniques in LTE



(b) 3GPP Release-11 FeICIC with reduced power ABS (RP-ABS).
Fig. 2. LTE-Advanced frame structures for time-domain ICIC.

and LTE-Advanced [12]–[14]. 3GPP Release-10 introduced a time-domain based enhanced ICIC (eICIC). It uses almost blank subframes (ABS) which requires the MBS to completely blank the transmit power on the physical downlink shared channel (PDSCH) resource elements as shown in Fig. 2(a). This separates the radio frames into coordinated subframes (CSF) and uncoordinated subframes (USF). 3GPP Release-11 defines further-enhanced ICIC (FeICIC), where the data on PDSCH is still transmitted but at a reduced power level as shown in Fig. 2(b).

The MBSs can schedule their UEs either in USF or in CSF based on the scheduling threshold ρ . Similarly, the UABSs can schedule their UEs either in USF or in CSF based on the scheduling threshold ρ' . Let β denote the USF duty cycle, defined as the ratio of number of USF subframes to total number of subframes in a radio frame. Then, the duty cycle of CSFs is $(1 - \beta)$. For ease of simulation, the USF duty cycle β is fixed at 50% in this paper for all the MBSs, which is shown in [7] to have limited effect on system performance when ρ and ρ' are optimized. Finally, let $0 \leq \alpha \leq 1$ denote the power reduction factor in coordinated subframes of the MBS for the FeICIC technique; $\alpha = 0$ corresponds to Release-10 eICIC, while $\alpha = 1$ corresponds to no ICIC.

Given the eICIC and FeICIC framework in 3GPP LTE-Advanced as in Fig. 2, and following an approach similar to that in [7] for a HetNet scenario, the signal-to-interference ratio (SIR) experienced by an arbitrary UE can be defined for CSFs and USFs for the MOI and the UOI as follows:

$$\Gamma = \frac{S_{\text{mbs}}(d_{mn})}{S_{\text{uabs}}(d_{un}) + Z}, \rightarrow \text{USF SIR from MOI} \quad (2)$$

$$\Gamma_{\text{csf}} = \frac{\alpha S_{\text{mbs}}(d_{mn})}{S_{\text{uabs}}(d_{un}) + Z} \rightarrow \text{CSF SIR from MOI}, \quad (3)$$

$$\Gamma' = \frac{S_{\text{uabs}}(d_{un})}{S_{\text{mbs}}(d_{mn}) + Z} \rightarrow \text{USF SIR from UOI}, \quad (4)$$

$$\Gamma'_{\text{csf}} = \frac{S_{\text{uabs}}(d_{un})}{\alpha S_{\text{mbs}}(d_{mn}) + Z} \rightarrow \text{CSF SIR from UOI}, \quad (5)$$

where Z is the total interference power at a UE during USF or CSF from all the MBSs and UABSs, excluding the MOI and the UOI. In hexagonal grid UABS deployment model (and

in [7]), locations of the UABSs (and small cells) are fixed. In order to maximize the 5pSE of the network, we actively consider the SIRs in (2)–(5) while optimizing the locations of the UABSs using the genetic algorithm.

B. UE Association and Scheduling

The cell selection process relies on Γ and Γ' in (2) and (4), respectively, for the MOI and UOI SIRs, as well as the CRE τ . If $\tau\Gamma'$ is less than Γ , then the UE is associated with the MOI; otherwise, it is associated with the UOI. After cell selection, the MBS-UE (MUE) and UABS-UE (UUE) can be scheduled either in USF or in CSF radio subframes as:

$$\text{If } \Gamma > \tau\Gamma' \text{ and } \Gamma \leq \rho \rightarrow \text{USF} - \text{MUE}, \quad (6)$$

$$\text{If } \Gamma > \tau\Gamma' \text{ and } \Gamma > \rho \rightarrow \text{CSF} - \text{MUE}, \quad (7)$$

$$\text{If } \Gamma \leq \tau\Gamma' \text{ and } \Gamma' > \rho' \rightarrow \text{USF} - \text{UUE}, \quad (8)$$

$$\text{If } \Gamma \leq \tau\Gamma' \text{ and } \Gamma' \leq \rho' \rightarrow \text{CSF} - \text{UUE}. \quad (9)$$

Once a UE is assigned to an MOI/UOI, and it is scheduled within a USF/CSF, then the SE for this UE can be expressed for the four different scenarios in (6)–(9) as follows:

$$C_{\text{usf}}^{\text{mbs}} = \frac{\beta \log_2(1 + \Gamma)}{N_{\text{usf}}^{\text{mbs}}}, \quad (10)$$

$$C_{\text{csf}}^{\text{mbs}} = \frac{(1 - \beta) \log_2(1 + \Gamma_{\text{csf}})}{N_{\text{csf}}^{\text{mbs}}}, \quad (11)$$

$$C_{\text{usf}}^{\text{uabs}} = \frac{\log_2(1 + \Gamma')}{N_{\text{usf}}^{\text{uabs}}}, \quad (12)$$

$$C_{\text{csf}}^{\text{uabs}} = \frac{\log_2(1 + \Gamma'_{\text{csf}})}{N_{\text{csf}}^{\text{uabs}}}, \quad (13)$$

where $N_{\text{usf}}^{\text{mbs}}$, $N_{\text{csf}}^{\text{mbs}}$, $N_{\text{usf}}^{\text{uabs}}$, and $N_{\text{csf}}^{\text{uabs}}$ are the number of MUEs and UUEs scheduled in USF and CSF radio subframes, and Γ , Γ_{csf} , Γ' , Γ'_{csf} are as in (2)–(5). We utilize the 5pSE defined as $C_{5\text{th}}(\mathbf{X}_{\text{uabs}}, \mathbf{S}_{\text{ICIC}})$ that relies on UABS locations and ICIC parameters, where \mathbf{S}_{ICIC} denotes a $N_{\text{uabs}} \times 4$ matrix that includes the ICIC parameters $\tau, \alpha, \rho, \rho'$ in its each row for a given UABS. In particular, the 5pSE corresponds to the worst fifth percentile UE capacity among the capacities of all the N_{ue} UEs (calculated based on (10)–(13)) within the simulation area, and we believe it is a critical metric for PSC scenarios to maintain a minimum QoS level at all UEs.

III. UABS DEPLOYMENT OPTIMIZATION

The cell-edge user SE is defined as 5pSE of the cumulative distribution function of the user throughput. And the 5pSE is a metric to measure the performance of a network. In this section, we discuss the UABS deployment using the genetic algorithm (GA) and the hexagonal grid model, where we use the 5pSE as an optimization metric to maximize for both scenarios.

A. Genetic Algorithm based UABS Deployment Optimization

The GA is a population-based optimization technique that can search a large environment simultaneously to reach an optimal solution [6]. In this paper, the UABS coordinates and the ICIC parameters constitute the GA population and

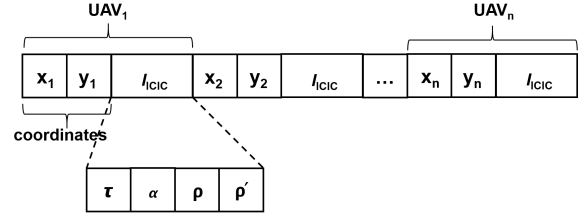


Fig. 3. An example of a chromosome for FeICIC simulation, where the UABS locations, ICIC parameter τ , α , ρ , and ρ' are optimized. The ICIC parameter β is not optimized and is fixed at 50% duty cycle.

a subsequent chromosome is illustrated in Fig. 3. Listing 1 describes the main steps used to optimize the UABS locations and ICIC parameters while computing the 5pSE.

Listing 1. Steps for optimizing population using GA.

```

Input:
Population: set of UABS locations and ICIC parameters
FITNESS function: 5pSE of the network
Output:
Args: Best individuals of ICIC parameters and highest 5pSE
Method:
NewPopulation ← empty set
StopCondition: Number of iterations
SELECTION: Roulette wheel selection method
while (! StopCondition)
{
  for i = 1 to Size do
  {
    Parent1 ← SELECTION(NewPopulation, FITNESS function)
    Parent2 ← SELECTION(NewPopulation, FITNESS function)
    Child ← Reproduce(Parent1, Parent2)
    if (small random probability)
    {
      child ← MUTATE(Child)
      add child to NewPopulation
    }
  }
  EVALUATE(NewPopulation, FITNESS function);
  Args ← GetBestSolution(NewPopulation)
  Population ← Replace(Population, NewPopulation)
}

```

We apply the GA to simultaneously optimize the UABS locations and ICIC parameters in order to maximize the 5pSE of the network over a given geographical area of interest. The location of each UABS within a rectangular simulation area is given by (x_i, y_i) where $i \in \{1, 2, \dots, N_{\text{uabs}}\}$. The UABS locations and the ICIC parameters that maximize the 5pSE objective function can be calculated as

$$[\hat{\mathbf{X}}_{\text{uabs}}, \hat{\mathbf{S}}_{\text{ICIC}}] = \arg \max_{\mathbf{X}_{\text{uabs}}, \mathbf{S}_{\text{ICIC}}} C_{5\text{th}}(\mathbf{X}_{\text{uabs}}, \mathbf{S}_{\text{ICIC}}). \quad (14)$$

Since searching for optimal \mathbf{X}_{uabs} and \mathbf{S}_{ICIC} through a brute force approach is computationally prohibitive, in this paper we use the GA to find optimum UABS locations and the best-fit ICIC parameters τ , α , ρ , and ρ' for each UABS.

B. UABS Deployment on a Hexagonal Grid

As a lower complexity alternative to optimizing UABS locations, we consider deploying the UABSs on a hexagonal grid, where the position of the UABSs are deterministic. We assume that the UABSs are placed within the rectangular simulation area regardless of the existing MBS locations. The 5pSE for this network is determined by using a brute

TABLE I. Simulation parameters.

Parameter	Value
MBS and UE intensity	4 per km ² and 100 per km ²
MBS and UABS transmit powers	46 dBm and 30 dBm
Path-loss exponent	4
Altitude of UABSs	121.92 m (400 feet)
Simulation area	10 × 10 km ²
GA population size and generation number	60 and 100
GA crossover and mutation probabilities	0.7 and 0.1
Cell range expansion (τ) in dB	0 to 15 dB
Power reduction factor for MBS during (α)	0 to 1
Duty cycle for the transmission of USF (β)	0.5 or 50%
Scheduling threshold for UUEs (ρ)	20 dB to 40 dB
Scheduling threshold for MUEs (ρ')	-20 dB to -10 dB
MBS destroyed sequence	50% and 97.5%
PSC LTE Band 14 center frequency	763 MHz for downlink and 793 MHz for uplink

force technique as described in the pseudo-code 2 which only considers optimization of the ICIC parameters captured through the matrix \mathbf{S}_{ICIC} . The optimized ICIC parameters that maximize the 5pSE can then be calculated as:

$$\hat{\mathbf{S}}_{\text{ICIC}} = \arg \max_{\mathbf{S}_{\text{ICIC}}} C_{5\text{th}}(\mathbf{X}_{\text{uabs}}^{(\text{hex})}, \mathbf{S}_{\text{ICIC}}), \quad (15)$$

where $\mathbf{X}_{\text{uabs}}^{(\text{hex})}$ are the fixed hexagonal locations of the deployed UABSs within the simulation area.

Listing 2. Steps for computing 5pSE for hexagonal grid deployment.

```

Input: set of UABS locations and ICIC parameters
Output: SE: 5pSE for the network
Method:
StopCondition: Number of iterations
while(! StopCondition)
{
  Generate UABS locations
  for t = 1 to ICICParams.tau[t] do
  {
    for a = 1 to ICICParams.alpha[a] do
    {
      for r = 1 to ICICParams.rho[r] do
      {
        for p = 1 to ICICParams.rhoprime[p] do
        {
          SE = Calc5thPercentileSE(nodal locations, nodal
            Tx powers, path-loss, tau, beta, alpha,
            rho, rhoprime)
        }
      }
    }
  }
}

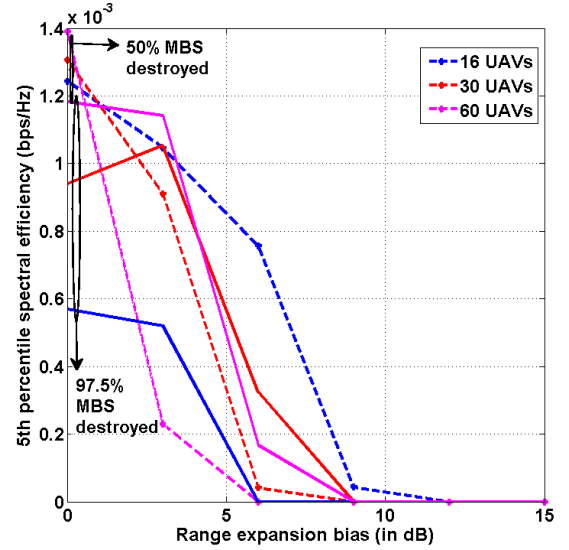
```

IV. SIMULATION RESULTS

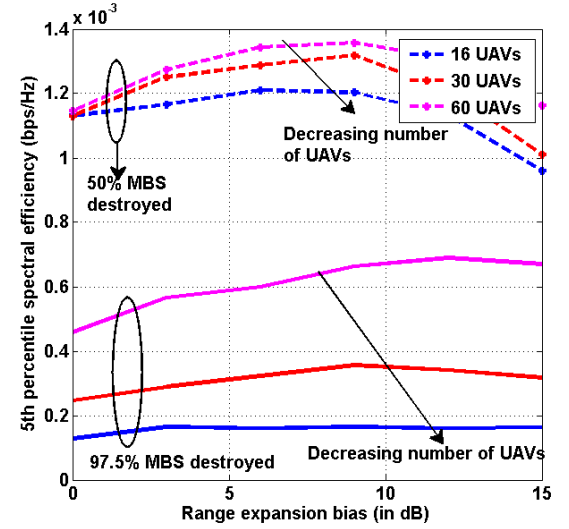
In this section, using computer simulations, we compare the 5pSE with and without ICIC techniques while considering different UABS deployment strategies. Unless otherwise specified, the system parameters for the simulations are set to the values in Table I.

A. 5pSE with UABSs Deployed on a Hexagonal Grid

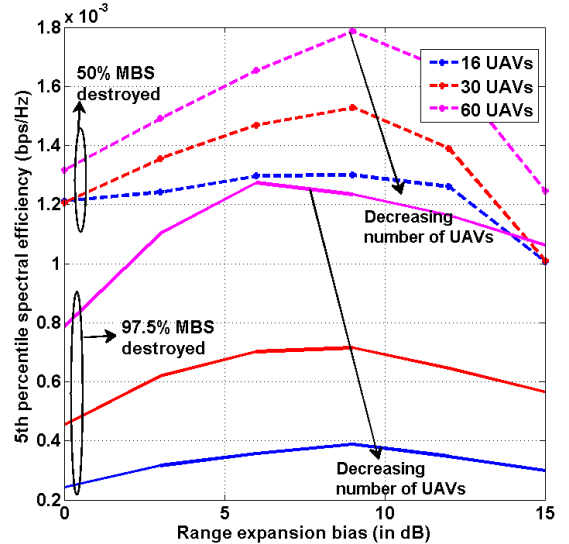
The variations in 5pSE with respect to CRE, when the UABSs are deployed on a hexagonal grid and utilizing optimized ICIC parameters (see (15) and Listing 2) are shown in Fig. 4. With no CRE, the number of UEs associated with the UABSs and the interference experienced by these UEs is



(a) 5pSE without any ICIC.



(b) 5pSE with eICIC.



(c) 5pSE with FeICIC.

Fig. 4. 5pSE versus CRE for eICIC and FeICIC techniques, when the UABSs are deployed on a hexagonal grid.

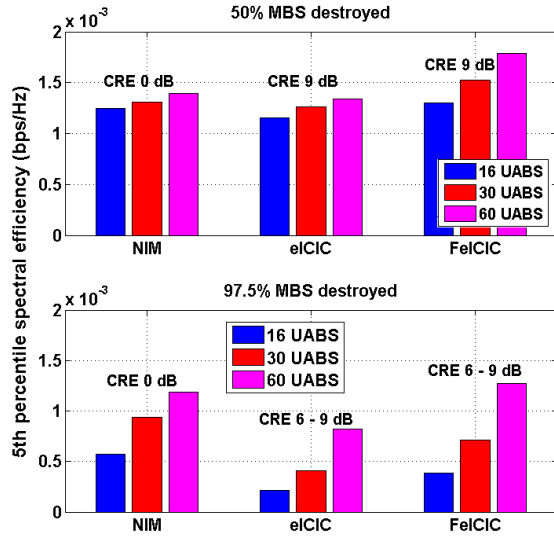


Fig. 5. Peak observations for the 5pSE, when the UABS are deployed on a fixed hexagonal grid.

minimal. With the no-ICIC mechanism (NIM) the peak value for the 5pSE is observed at around 0 dB CRE as seen in Fig. 4(a). On the other hand, the 5pSE for ICIC techniques at 0 dB CRE are relatively lower as seen in Fig. 4(b) and Fig. 4(c), due to blank subframes at the MBSs for eICIC, and power reduction of the CSFs at the MBSs for FeICIC.

As the CRE increases, the number of UEs associated with the UABSs increases and so does the interference experienced by these UEs. Hence, with NIM the 5pSE decreases with increasing CRE as seen in Fig. 4(a). On the other hand, the ICIC techniques observe improvement in SE performance. The peak values of the 5pSE for the ICIC techniques is observed when the CRE is between 6 – 9 dB. This influence of CRE on the 5pSE for NIM and ICIC is summarized in Fig. 5.

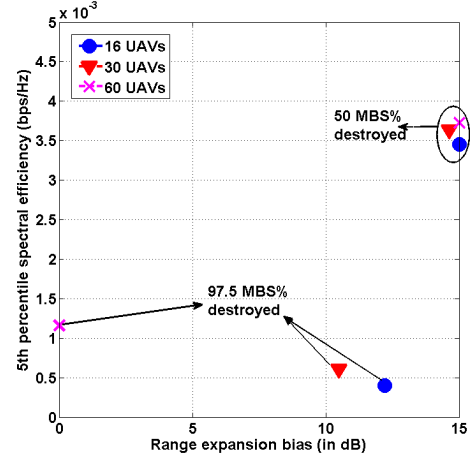
Overall, the 5pSE for the network is higher when larger numbers of UABSs are deployed and when fewer MBSs are destroyed. Also, the 5pSE decreases with the increasing number of destroyed MBSs as seen in Fig. 4.

B. 5pSE with GA Based UABS Deployment Optimization

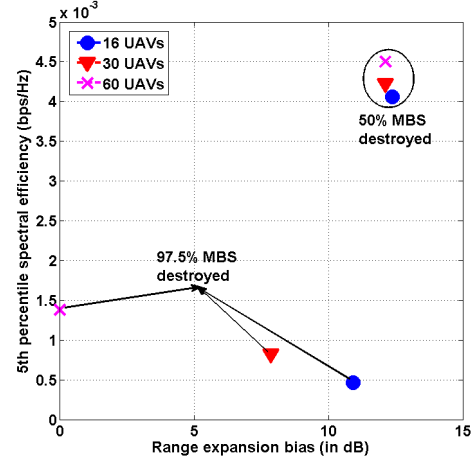
Using the UABS locations and ICIC parameters optimized through the GA as in (14) and Listing 1, we plot the peak 5pSE for the network with respect to the optimized CRE value in Fig. 6. In the GA based simulations, the optimum CRE value is directly related to the locations of the UABSs with respect to the MBSs, the number of UEs offloaded to the UABSs, and the amount of interference observed by the UEs.

Consider first that the 50% of the MBSs are destroyed, which implies that there are still a large number of MBSs present and the interference from these MBSs is substantial. Hence, offloading a large number of UEs from MBSs to UABSs with higher values of CRE and ICIC is necessary in achieving better 5pSE gains as shown in Fig. 6(a) and Fig. 6(b) for eICIC and FeICIC, respectively.

When most of the infrastructure is destroyed (i.e., when 97.5% of the MBSs destroyed), the interference observed from the MBSs is limited and a larger number of UEs need to be



(a) 5pSE with eICIC.



(b) 5pSE with FeICIC.

Fig. 6. Peak 5pSE versus optimized CRE for eICIC and FeICIC techniques, when the UABS locations and ICIC parameters are optimized using the GA.

served by the UABSs. Therefore, with fewer UABSs deployed, higher CRE are required to serve larger number of UEs and achieve better 5pSE. On the other hand, when larger number of UABSs are deployed, smaller values of CRE will result in better 5pSE gains. We record these behavior in Fig. 6(a) and Fig. 6(b) for eICIC and FeICIC, respectively.

C. Performance Comparison Between Fixed (Hexagonal) and Optimized UABS Deployment with eICIC and FeICIC

We summarize our key results from earlier simulations in Fig. 7 to compare the key trade-offs between fixed (hexagonal) deployment and GA based deployment of UABSs. The comparison of Fig. 4 and Fig. 6 show that the optimized deployment of UABSs provides a better 5pSE than the UABSs deployed on a fixed hexagonal grid, which are also reflected into the comparative analysis in Fig. 7 which considers an optimized CRE. Moreover, Fig. 7 shows that the 5pSE gains from the optimization of UABS locations are more significant when 50% of the MBSs are destroyed and less significant when 97.5% of the MBSs are destroyed.

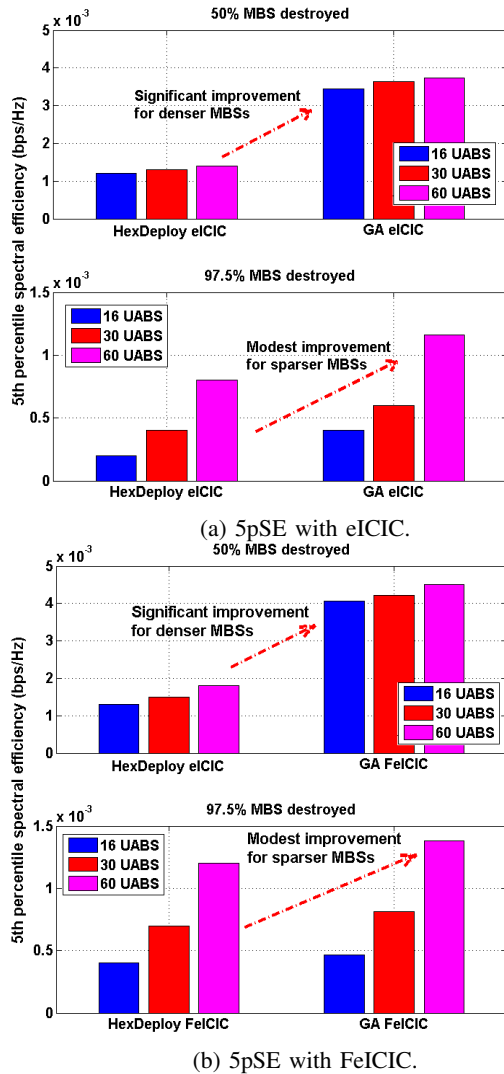


Fig. 7. 5pSE comparisons for eICIC and FeICIC techniques, when the UABS locations are optimized using the GA and when the UABSs are deployed in a fixed hexagonal grid.

When 50% MBSs are destroyed, there are still a large number of MBSs present which cause substantial interference. Hence, in such interference driven scenario it is important to optimize the locations of the UABSs, and use of larger number of UABSs provide only marginal gains in the 5pSE.

On the other hand, with 97.5% of the MBSs destroyed, the interference from the MBSs is small, and deploying the UABSs on a hexagonal grid will perform close to optimum UABS deployment. The difference between the hexagonal deployment and optimized deployment is especially small for the FeICIC scenario where power reduction factor α in the MBS CSFs provides an additional optimization dimension for improving the 5pSE. Use of larger number of UABSs when 97.5% of the MBSs are destroyed is also shown to provide significant gains in the 5pSE, in contrast to modest gains in the 5pSE when 50% of the MBSs are destroyed.

V. CONCLUDING REMARKS

In this article, we show that the mission-critical communications could be maintained by deploying UABSs in

the event of any damage to the public safety infrastructure. Through simulations, we compare and analyze the 5pSE for the network when the UABSs are deployed on a hexagonal grid and when placed optimally using the GA. Our analysis show that deployment of the UABSs on a hexagonal grid is close to optimal when the observed interference is limited. In the presence of substantial interference, the GA approach is more effective for deploying UABSs. Finally, we observe that the HetNets, with reduced power subframes (FeICIC) yields better 5pSE than that with almost blank subframes (eICIC). Future research directions include optimizing the UABS locations using learning techniques and developing a path-planning algorithm for UABS placement.

ACKNOWLEDGMENT

This research was supported in part by NSF under the grants AST-1443999 and CNS-1453678. The authors would like to thank A. Merwaday for his useful feedback.

REFERENCES

- [1] A. Kumbhar, F. Koohifar, I. Guvenc, and B. Mueller, "A survey on legacy and emerging technologies for public safety communications," *IEEE Commun. Survey Tuts.*, vol. 18, pp. 97–124, Sept. 2016.
- [2] D. Athukoralage, I. Guvenc, W. Saad, and M. Bennis, "Regret based learning for UAV assisted LTE-U/WiFi public safety networks," in *Proc. IEEE Global Commun. Conf. (GLOBECOM)*, Washington, DC, Dec. 2016, pp. 1–7.
- [3] J. Atkinson, "Motorola Solutions and EE confirmed for new UK Emergency Services Network," *Wireless Magazine*, Dec. 2015.
- [4] M. Hainzl, "Integrating UAVs into Public Safety LTE Networks," Tech. Rep., 2014.
- [5] L. K. Moore, *The first responder network (FirstNet) and next-generation communications for public safety: Issues for congress*. Congressional Research Service, 2014.
- [6] A. Merwaday, A. Tuncer, A. Kumbhar, and I. Guvenc, "Improved Throughput Coverage in Natural Disasters: Unmanned Aerial Base Stations for Public-Safety Communications," *IEEE Vehic. Technol. Mag.*, vol. 11, no. 4, pp. 53–60, Dec. 2016.
- [7] A. Merwaday, S. Mukherjee, and I. Guvenc, "Capacity analysis of LTE-Advanced HetNets with reduced power subframes and range expansion," *EURASIP J. Wireless Commun. Netw.*, no. 1, pp. 1–19, Nov. 2014.
- [8] K. Gomez, S. Kandeepan, M. M. Vidal, V. Boussemart, R. Ramos, R. Hermenier, T. Rasheed, L. Goratti, L. Reynaud, D. Grace, Q. Zhao, Y. Han, S. Rehan, N. Morozs, I. Bucaille, T. Wirth, R. Campo, and T. Javornik, "Aerial base stations with opportunistic links for next generation emergency communications," *IEEE Commun. Mag.*, vol. 54, no. 4, pp. 31–39, 2016.
- [9] K. Gomez, T. Rasheed, L. Reynaud, and S. Kandeepan, "On the performance of aerial LTE base-stations for public safety and emergency recovery," in *Proc IEEE Globecom Workshops (GC Wkshps)*, Atlanta, GA, 2013, pp. 1391–1396.
- [10] Y. Wang, C. Yin, and R. Sun, "Hybrid Satellite-Aerial-Terrestrial Networks for Public Safety," in *Proc. Intl. Conf. Personal Satellite Services. Next-Generation Satellite Nwk and Commun. Systems*. Genoa, Italy: Springer, July 2016, pp. 106–113.
- [11] R. K. Ganti, F. Baccelli, and J. G. Andrews, "A new way of computing rate in cellular networks," in *Proc. IEEE Int. Conf. Commun. (ICC)*, Kyoto, Japan, June 2011, pp. 1–5.
- [12] H. Holma, A. Toskala, and J. Reunanen, *LTE Small Cell Optimization: 3GPP Evolution to Release 13*. John Wiley & Sons, Jan. 2016.
- [13] B. Soret and K. I. Pedersen, "Macro transmission power reduction for hetnet co-channel deployments," in *Proc. IEEE Global Commun. Conf. (GLOBECOM)*, Anaheim, CA, Dec. 2012, pp. 4126–4130.
- [14] M. S. Ali, "An Overview on Interference Management in 3GPP LTE-Advanced Heterogeneous Networks," *Int. J. Future Generation Commun. Netw.*, vol. 8, no. 1, pp. 55–68, June 2015.